

---

This is an electronic reprint of the original article.  
This reprint may differ from the original in pagination and typographic detail.

Jokinen, Ville; Kankuri, Esko; Hoshian, Sasha; Franssila, Sami; Ras, Robin  
**Superhydrophobic blood-repellent surfaces**

*Published in:*  
Advanced Materials

*DOI:*  
[10.1002/adma.201705104](https://doi.org/10.1002/adma.201705104)

Published: 01/06/2018

*Document Version*  
Publisher's PDF, also known as Version of record

*Published under the following license:*  
CC BY-NC

*Please cite the original version:*  
Jokinen, V., Kankuri, E., Hoshian, S., Franssila, S., & Ras, R. (2018). Superhydrophobic blood-repellent surfaces. *Advanced Materials*, 30(24), Article 1705104. <https://doi.org/10.1002/adma.201705104>

---

This material is protected by copyright and other intellectual property rights, and duplication or sale of all or part of any of the repository collections is not permitted, except that material may be duplicated by you for your research use or educational purposes in electronic or print form. You must obtain permission for any other use. Electronic or print copies may not be offered, whether for sale or otherwise to anyone who is not an authorised user.

# Superhydrophobic Blood-Repellent Surfaces

Ville Jokinen,\* Esko Kankuri,\* Sasha Hoshian, Sami Franssila, and Robin H. A. Ras\*

Superhydrophobic surfaces repel water and, in some cases, other liquids as well. The repellency is caused by topographical features at the nano-/micro-scale and low surface energy. Blood is a challenging liquid to repel due to its high propensity for activation of intrinsic hemostatic mechanisms, induction of coagulation, and platelet activation upon contact with foreign surfaces. Imbalanced activation of coagulation drives thrombogenesis or formation of blood clots that can occlude the blood flow either on-site or further downstream as emboli, exposing tissues to ischemia and infarction. Blood-repellent superhydrophobic surfaces aim toward reducing the thrombogenicity of surfaces of blood-contacting devices and implants. Several mechanisms that lead to blood repellency are proposed, focusing mainly on platelet antiadhesion. Structured surfaces can: (i) reduce the effective area exposed to platelets, (ii) reduce the adhesion area available to individual platelets, (iii) cause hydrodynamic effects that reduce platelet adhesion, and (iv) reduce or alter protein adsorption in a way that is not conducive to thrombus formation. These mechanisms benefit from the superhydrophobic Cassie state, in which a thin layer of air is trapped between the solid surface and the liquid. The connections between water- and blood repellency are discussed and several recent examples of blood-repellent superhydrophobic surfaces are highlighted.

occlusion or compromise graft functionality and valves that can be implanted using minimally invasive endovascular or transcatheter procedures.<sup>[3]</sup> Although several advances have set major milestones and made breakthroughs in treatment, overcoming the various levels of blood incompatibility of surfaces and their propensity to adsorb proteins and instigate both enzyme cascade and blood-cell activations remains an unsolved issue.<sup>[4,5]</sup> These early host protein–material interactions, the dynamics of which are known as the Vroman effect, occur in a qualitative and time-dependent manner and lead to activation of blood cells, inflammation, and thrombosis. Especially, thrombosis, blood clotting early or late after implantation, is a severe concern for medical devices and materials in contact with blood. Material-activated or adherent platelets as well as material-activated coagulation factors or material-inhibited anticoagulation factors or cascades can instigate formation of thrombi that obstruct blood flow either

## 1. Introduction

When medical devices come into contact with blood, the interaction poses a threat of undesired activation of blood cells (such as platelets and monocyte/macrophages of the immune system) or other bioactive blood components (such as the complement and coagulation cascades). These reactions can lead to formation of blood clots or thrombi, inflammation, or a more widespread, prolonged activation of the immune system.<sup>[1,2]</sup> Advances in cardiovascular materials and engineering have produced improved artificial vascular grafts, as well as drug-eluting stents to reduce the adverse responses that drive graft

at the site of the implant or even further downstream in the circulation.<sup>[6]</sup> Clots released from the thrombi can travel with the bloodstream and occlude (embolize) downstream vessels, leading to inflammation, ischemia, infarction, and eventually irreversible tissue damage. An inflammation-promoting or proinflammatory material–cell microenvironment may cause or sensitize platelets to activating prothrombotic stimuli.<sup>[7]</sup> Thus, material adherence or material-induced activation of other blood components, such as leukocytes or latent protein complexes, promotes innate immunity responses (immunothrombosis), which then either directly or indirectly further platelet activation.<sup>[8]</sup> Importantly, even factors unrelated to the

Dr. V. Jokinen, Dr. S. Hoshian, Prof. S. Franssila  
Department of Chemistry and Materials Science  
School of Chemical Engineering  
Aalto University  
Tietotie 3, Micronova, 02150 Espoo, Finland  
E-mail: ville.p.jokinen@aalto.fi

 The ORCID identification number(s) for the author(s) of this article can be found under <https://doi.org/10.1002/adma.201705104>.

© 2018 The Authors. Published by WILEY-VCH Verlag GmbH & Co. KGaA, Weinheim. This is an open access article under the terms of the Creative Commons Attribution-NonCommercial License, which permits use, distribution and reproduction in any medium, provided the original work is properly cited and is not used for commercial purposes.

The copyright line for this article was changed on 6 Apr 2018 after original online publication.

DOI: 10.1002/adma.201705104

Dr. E. Kankuri  
Department of Pharmacology  
Faculty of Medicine  
University of Helsinki  
Haartmaninkatu 8, PO Box 63, Biomedicum, 00014 Helsinki, Finland  
E-mail: esko.kankuri@helsinki.fi

Prof. R. H. A. Ras  
Department of Applied Physics  
School of Science  
Aalto University  
Puumiehenkuja 2, 02150 Espoo, Finland  
E-mail: robin.ras@aalto.fi

Prof. R. H. A. Ras  
Department of Bioproducts and Biosystems  
School of Chemical Engineering  
Aalto University  
Kemistintie 1, 02150 Espoo, Finland

material itself, such as altered blood-flow parameters (rheology) or turbulent flow, can lead to platelet activation.<sup>[9,10]</sup> Thrombosis can effectively be counteracted by various antithrombotic drugs, but therapy is associated with major bleeding complications and increased mortality as a tradeoff.<sup>[11]</sup> Activation of the inflammatory response and tissue remodeling can lead to further vessel constriction through, for example, activation of cells of the vascular wall, smooth muscle cells in particular, to proliferate and form extensive scar tissue in the vessel wall. Moreover, inflammation in general is associated with thrombosis by shifting the homeostatic balance between clotting and fibrinolysis.<sup>[12,13]</sup>

Various platelet surface molecules mediate platelet activation, adhesion, and platelet–material interactions. These include the platelet adhesion receptors (glycoprotein [GP] Ib-IX-B, immunoreceptor tyrosine-based activation motif [such as Fc receptor gamma chain and the collagen receptor GPVI]), pattern recognition receptors (such as Toll-like receptors, nucleotide-binding oligomerization domain-like receptors or the receptors for advanced glycation end products) as well as the G-protein-coupled receptors (such as the protease-activated receptors). For more information on the mechanisms of platelet adhesion and activation by different surfaces and agents, the reader is referred to previous reviews.<sup>[14–16]</sup> Several of the platelet surface molecules act as druggable targets for prevention of platelet activation and aggregation, and the formation of thrombi.<sup>[17]</sup>

Unfortunately, current solutions are far from perfect. For example, smooth, passivated surfaces and bioactive coatings with heparin or other antithrombotic coagulant coatings have been used to prevent blood coagulation.<sup>[5]</sup> These grafted

coatings, however, eventually wear off over time and reveal the plain blood-incompatible surfaces, thus only delaying the onset of the problems. Traditionally smooth polymers with specific surface chemistries (both hydrophobic and hydrophilic have been studied) have been implicated to be most suitable for blood compatibility.<sup>[18,19]</sup> This is in contrast to the strategy reviewed herein, which focuses on extremely rough surfaces.

Here, we aim to provide the reader with the current understanding of the potential of micro- and nanostructured superhydrophobic (SHB) surfaces for blood-compatible medical devices. The concept is presented in **Figure 1**. For a broader perspective of applications of SHB surfaces for biomedical technology, the reader is pointed to recent reviews by Falde et al.<sup>[20]</sup> and Wen et al.<sup>[21]</sup>

## 2. Superhydrophobicity

SHB surfaces repel water to a great extent, as demonstrated by water beading up, and quantified by high advancing and receding contact angles ( $>150^\circ$ ). Contact angle hysteresis, i.e., the difference between the advancing and receding contact angle, is small for superhydrophobic surfaces, which leads to very low adhesion of water droplets and causes them to roll off the surfaces at low sliding angles. Droplets on SHB surfaces sit on a cushion of air (called the plastron) trapped between the micro- and/or nanosized surface structures. This is called the Cassie (or Cassie–Baxter) state of wetting (**Figure 2a**). The Wenzel state (**Figure 2b**) also has high contact angles, but the hysteresis and the sliding angles are high, and often the

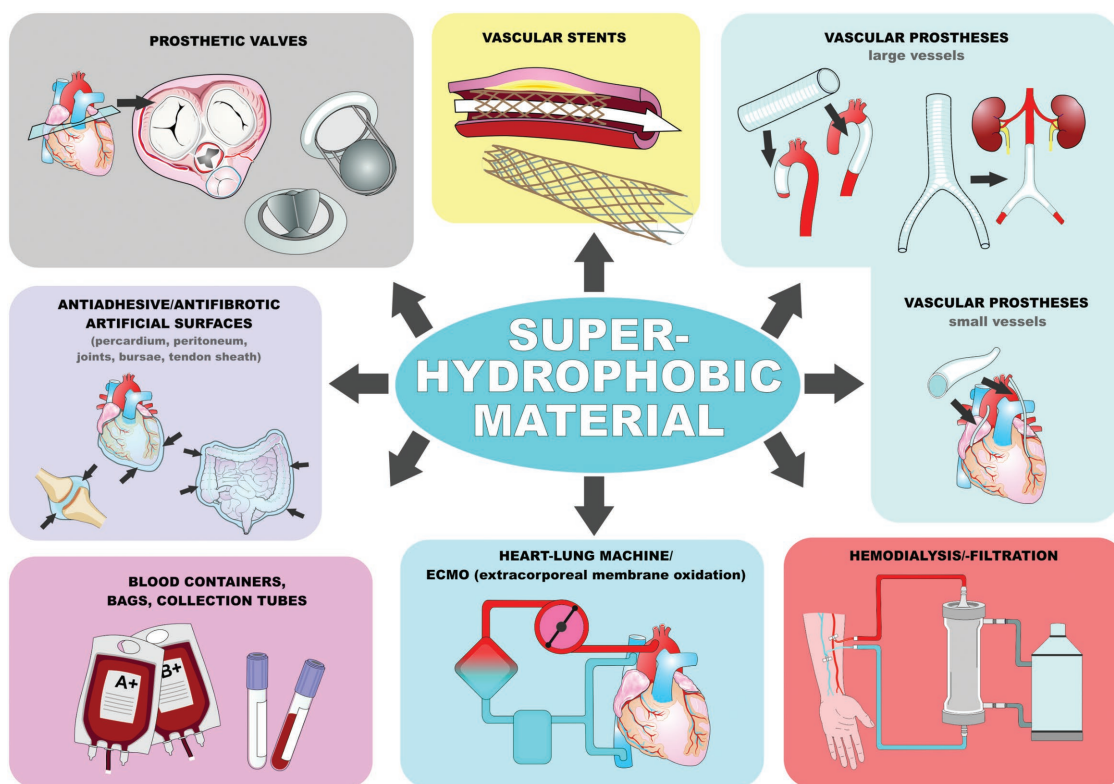


**Figure 1.** The concept of utilizing superhydrophobic surfaces as blood-repellent coatings for medical devices.

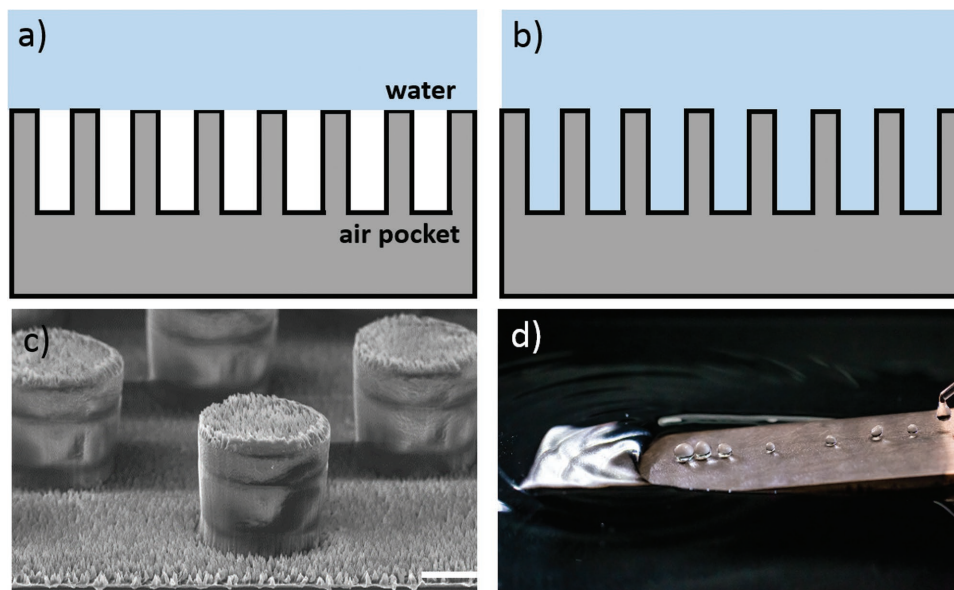


**Figure 2.** Superhydrophobic surfaces. a) The Cassie state (superhydrophobic). b) The Wenzel state (not superhydrophobic). c) Example of a dual-scale roughness superhydrophobic surface. The scale bar is 4  $\mu\text{m}$ . c) Adapted with permission.<sup>[23]</sup> Copyright 2013, Elsevier. d) Water droplets rolling off a superhydrophobic surface (The photograph in (d) is copyright of and used with the permission of Mika Latikka).

droplets adhere even at a tilt of  $180^\circ$ . For a recent review on basics of superhydrophobicity, the reader is referred to ref. [22].

Superhydrophobicity is achieved by surface roughness at the nano- and/or microscale combined with low-surface-energy chemistry, typically by hydrocarbon or fluorocarbon coatings. A nanostructured superhydrophobic surface can be pictured as a Fakir's bed, with the only contact to water droplets at the nail tips. The surface fraction of solid can be well below 10%. Figure 2c shows a dual micro-/nanoscale superhydrophobic surface made by hot-embossing a fluoropolymer material.<sup>[23]</sup> The point-like solid–liquid contact is the basis of many proposed mechanisms of blood repellency: a smaller contact area between cells and solid surface leads to reduced adhesion and mismatch between the surface structure size and platelet size prevents adhesion, too. However, the mechanical durability of SHB surfaces has been a key weakness that is currently being addressed by the community.<sup>[24,25]</sup>

Figure 2d shows water droplets on an SHB surface. The droplets are almost perfectly spherical due to surface tension, since both the advancing and the receding contact angles are high, and the adhesion to the surface is minimal. An alternative water-repellent state is achieved by the slippery liquid infused porous surfaces (SLIPS) approach, in which a porous surface is covered by an immiscible perfluorocarbon liquid.<sup>[26]</sup> Unlike SHB surfaces, the contact angles and the hysteresis are both low.

In general, when water flows over a solid surface, the liquid velocity can be approximated to zero at the liquid–solid interface. However, this assumption is not valid for SHB surfaces due to slippage caused by the air pocket. On a hierarchical microsurface–nanosurface, the slip length can be more than 400  $\mu\text{m}$ .<sup>[27]</sup> Because of the slip, the shear stress and drag are reduced at an SHB surface in both laminar and turbulent regimes.<sup>[28]</sup> This phenomenon is key in the self-cleaning

property of SHB surfaces. A large slip length can enhance micrometer-scale diffusion–osmosis by orders of magnitude.<sup>[29]</sup>

### 3. Micro- and Nanostructure-Induced Blood-Repellency

Micro- and/or nanostructures have been proposed to reduce platelet adhesion and thrombogenicity through various mechanisms. The most promising mechanisms are summarized in Table 1 and depicted in Figure 3. The range of materials, surface chemistries, size ranges, and topographical patterns tested is wide, which explains the multitude of mechanisms found in the literature. The mechanisms discussed here are related to surface micro- and nanostructures in general,

**Table 1.** Mechanisms of micro- and nanostructure-induced platelet antiadhesion.

Mechanism	Comments	References
1. Effective area (Figure 3a)	Blood platelet adhesion is limited by the surface area accessible to platelets.	[30–35]
2. Adhesion area (Figure 3b)	Platelets adhere less strongly if there are no topographically uniform areas for attaching. Critical size 1–2 $\mu\text{m}$ range.	[30–34,36,37]
3. Hydrodynamics (Figure 3c)	The boundary layer near an SHB surface has lower shear and a macroscopic slip velocity, which can alter platelet-adhesion dynamics.	[32,37,38]
4. Protein adsorption (Figure 3d)	Less protein can be adsorbed due to shear effects. Conformation of key proteins is denatured on high-curvature surfaces.	[39–41]

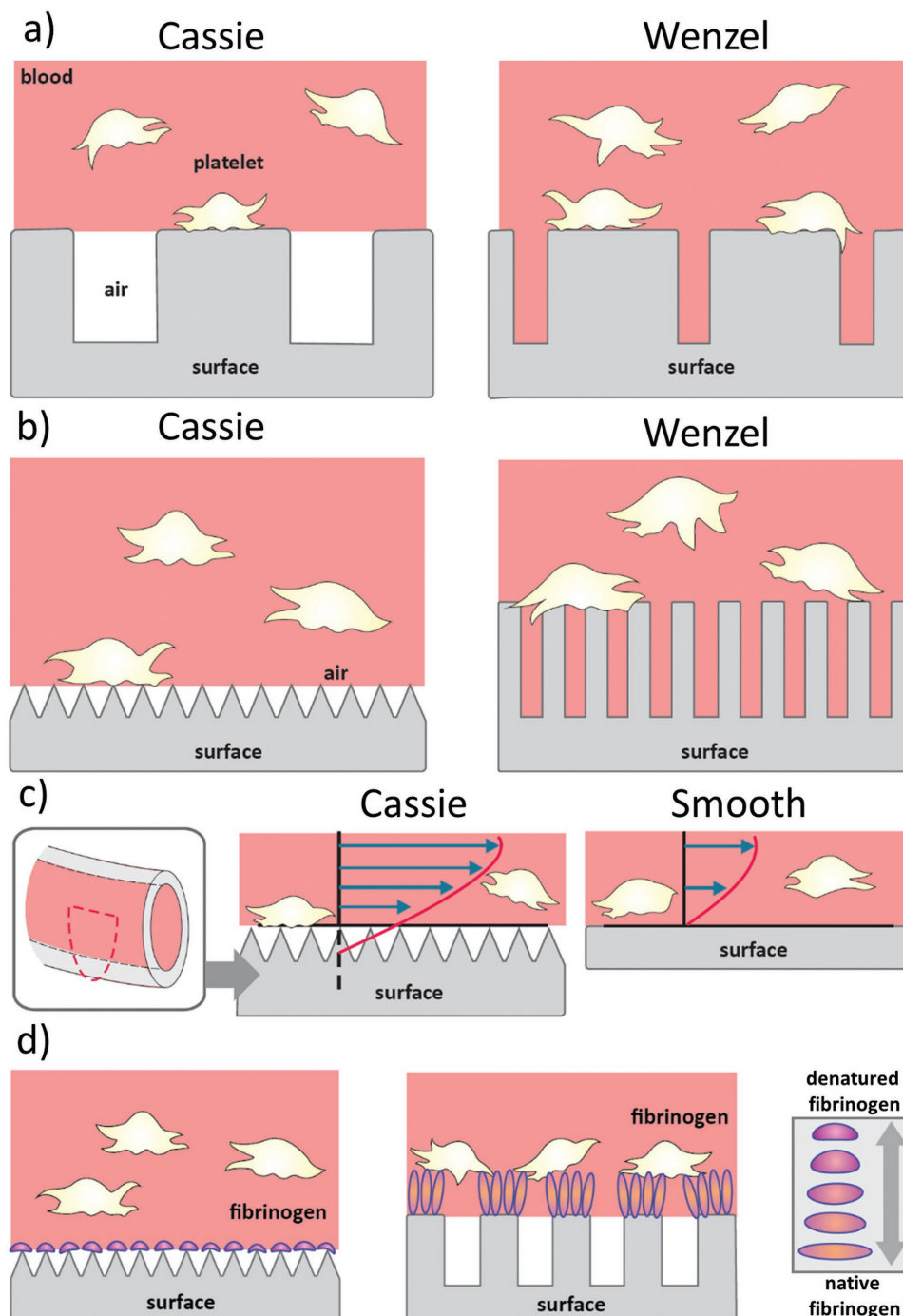


**Figure 3.** Mechanisms of micro- and nanostructure-induced blood repellency. a) Reduced effective surface area available to platelets in the Cassie state and Wenzel state. b) Reduced adhesion area available to individual platelets in the Cassie state and Wenzel state. c) Hydrodynamic effects on an SHB and a smooth surface. d) Protein-adsorption effects. A high radius of curvature leads to fibrinogen adsorbed in more denatured state, which is less conducive to platelet adhesion.<sup>[42]</sup>

superhydrophobic or not. The relationship of the various mechanisms to superhydrophobicity is discussed in the next section.

The total number of adherent platelets should correlate with the effective surface area accessible to the platelets. Hence, platelet adhesion can be reduced by limiting the effective area available to platelets (Figure 3a). One way to limit the effective

area is to utilize a superhydrophobic surface in the Cassie state.<sup>[30,35]</sup> Movafaghi et al.<sup>[30]</sup> showed that superhydrophobic titania nanotubes reduce the number of adherent platelets by up to 67% compared to nontextured surfaces, which was explained by a stable Cassie state leading to a smaller effective area. The activation levels were also reduced, as concluded

based on morphology investigation. The effective area also works in the other direction. Liquid on the same nanotube topography without the hydrophobic coating was in the Wenzel state. This means that there was more surface area accessible to platelets, and the number of platelets adhered was higher than on a smooth unstructured control. Moradi et al.<sup>[35]</sup> studied laser-ablated steel and titanium structures with hydrophilic and hydrophobic coatings. They found that a superhydrophobic cauliflower-like surface with a stable Cassie state (stable on immersion for over 6 d in water) was very resistant to platelet adhesion, while significantly more platelet adhesion was observed for a “triple pattern” topography that had a high contact angle but less stable Cassie state. The activation level of adhered platelets was also reduced based on morphology investigation.

A reduced effective area can also be achieved in the Wenzel state if the gaps between the structures are small enough so that the platelets cannot fit in-between, and only the tops of the features act as the effective surface area. There is some variance in the reported critical threshold values for the gaps, but they tend to lie just below the size of a platelet. Ding et al.<sup>[33]</sup> studied platelet penetration between TiO<sub>2</sub>-coated silicon pillars (rectangular lattice, height 2.5 μm, diameter range 0.5–6 μm, spacing range 0.5–16 μm) and concluded that the critical spacing threshold is between 1.5 and 3 μm. Milner et al.<sup>[32]</sup> utilized polyurethane nanopillars (rectangular lattice, either 700 nm for height, diameter, and separation, or 600 nm height and 400 nm diameter and separation). They concluded that a gap of ≈1.3 μm between adjacent pillars on the 700 nm high pillar sample was already too large and some platelets were able to penetrate the interpillar area. Koh et al.<sup>[34]</sup> utilized poly(lactic-co-glycolic acid) pillars of various dimensions and determined the critical spacing threshold to be 1 μm. The effective adhesion area can thus be reduced, either by ensuring a stable Cassie state or by utilizing spacing sizes in the 1–2 μm range, depending on the final details of the pattern. They also found that when the platelets only interacted with the tops of the pillars, the activation of the platelets was lower, as determined by flow cytometry of a marker targeting the glycoprotein IIb/IIIa complex.

A related mechanism is the size of uniform adhesion areas (Figure 3b) available to platelets in the Cassie state or the Wenzel state. Platelets adhere on solid surfaces, which means that if the surface does not have platelet-sized or larger uniform areas, the adhesion of the platelets is weaker.<sup>[30–34,36,37]</sup> This concept has been explained through the work of adhesion between platelets and a surface.<sup>[37]</sup> Chen et al.<sup>[36]</sup> proposed a division of the size ranges based on the size of platelets (2 μm) and the platelet pseudopods (50 nm). According to this division, a roughness larger than 2 μm would lead to increased adhesion of platelets; a roughness smaller than 50 nm would have no effect; and in between these values lies the promising range for antithrombogenicity.

Koh et al.<sup>[34]</sup> also argued that this effect can be enhanced on high-aspect-ratio flexible pillars that deform easily upon agitation, which can dislodge weakly adhered platelets. They also showed that platelets adhered only partially on solid surfaces tend to be less activated than platelets adhered on larger uniform solid areas.

In practice, micro- and nanostructures often lead to both reduced effective area and reduced adhesion area at the same

time, especially if nanostructures are used. For example, Sun et al.<sup>[31]</sup> reported a vertically aligned carbon nanotube forest with fluorinated polycarbonate urethanes and found that it almost completely eliminated the adhered platelets and also reduced the activation (glycoprotein IIb/IIIa complex) by 50% compared to a planar control. However, it is also feasible to fabricate structures that only exhibit one of these two features (Figure 3a,b), which can be utilized for studying the two effects independently.

The hydrodynamics are known to have a significant effect on platelet adhesion and thrombogenesis through altering collision frequencies, slip velocity, shear stress, and the concentration profiles of soluble proteins.<sup>[43,44]</sup> Hydrodynamic flow patterns can be significantly modified by micro- and nanostructures at the surface (Figure 3c). Fan et al.<sup>[37]</sup> studied the hydrodynamic effects on platelet adhesion on poly(dimethylsiloxane) (PDMS) surfaces with sub-micrometer parallel ridges (width = 500 nm, height = 100 nm) and nanoprotusions (≈40 nm), alone and in dual-scale combination. These were tested in a flow-cell setup at a shear rate of 1000 s<sup>-1</sup>, which is a typical arterial-wall shear rate.<sup>[45]</sup> They proposed that surface micro- and nanostructures increase slip flow rate at the boundary layer (the layer of liquid closest to the surface), which reduces the number of collisions between the platelets and the surface. Their experimental results showed that the dual-scale system had the least platelet adhesion, followed first by the larger ridge structures alone, then by the nanoprotusions alone, and finally by a planar surface. The dual-scale rough surfaces reduced the adhesion of platelets over fivefold compared to planar references and single-scale roughness.

Pham et al.<sup>[38]</sup> utilized hemispherical PDMS micropillars (radius 12–15 μm, height 0.9–2.7 μm, spacing 3–15 μm) in a flow-cell setup. These dimensions are in the same scale as the endothelial cell layer of blood vessels. Note that these dimensions are too big for effective-area and adhesion-area effects to come into play, so hydrodynamic effects were studied in isolation. They concluded that a high shear-stress difference between the top and the bottom of the microstructures was desirable. Depending on the exact structure, the shear stress at the top of the structures varied from 2.4 to 3.1 Pa, compared to 1.8 Pa shear stress obtained for planar control. The proposed mechanism was that the platelets that collide with the surface at the tops of the pillars do so at high shear rates, which might prevent adhesion. On the other hand, fewer platelets would tend to flow into the low-shear areas between the pillars. A reduction in the number of adhered platelets up to 78.4% was observed compared to the planar control.

Milner et al.<sup>[32]</sup> studied the effect of shear stress on platelet adhesion onto polyurethane nanopillars utilizing a rotating-disk setup. The shear stress across the sample varied from 0 to 6.7 Pa. The nanostructures significantly reduced platelet adhesion compared to a planar reference sample. However, the difference between the structured sample and the planar sample was only pronounced at lower shear stresses (<1 Pa). At high shear stresses, the adhesion on both the nanostructured and planar surfaces was minimal. They proposed that on the nanostructured surface lower shear stresses were able to detach colliding platelets since the adhesive forces were smaller due to the adhesion area effect.

Ramachandran et al.<sup>[46]</sup> compared ridge-like geometries for boundary-layer and shear-stress effects. Their conclusion from fluid dynamic simulations is that particles flow over the ridges and do not enter the valleys (50–100  $\mu\text{m}$  wide in their model), and therefore the platelets effectively have a smaller area with which to interact.

Superhydrophobic surfaces can reduce the amount of protein adsorption or cause the proteins to adsorb in an altered conformation (Figure 3d). Koc et al.<sup>[39]</sup> showed that, in static conditions, superhydrophobic surfaces with hydrocarbon or fluorocarbon surface chemistries adsorbed more albumin than their planar reference surfaces if the critical dimension was either 4  $\mu\text{m}$  or 800 nm and somewhat less if the critical dimension was 10 nm. However, under flow conditions, the albumin adsorption was greatly reduced on the structured surfaces and in the case of the 10 nm scale and the fluorocarbon chemistry, it was almost eliminated. The mechanism proposed is that the adhesion strength was smaller due to the size scale and, at the same time, the shear forces on the proteins on the superhydrophobic surfaces were higher due to the slip, which leads to enhanced desorption. This is a similar effect to that proposed for the platelets themselves (adhesion area effect and hydrodynamic effects) but on a smaller scale.

The topography and curvature of a surface can affect the denaturation of proteins upon adsorption. Roach et al.<sup>[40]</sup> studied bovine serum albumin and fibrinogen adsorption on nanoparticle surfaces of various sizes. As the radius of curvature decreased (i.e., smaller and sharper features), IR spectroscopy studies revealed that fibrinogen adsorbs in a more denatured state. Fibrinogen adsorbed on 10 nm feature sizes had lost nearly all of its initial  $\alpha$ -helical secondary structure into random coils, whereas fibrinogen adsorbed on 30 nm or larger critical dimension surfaces had nearly all of its  $\alpha$ -helical secondary structure intact. On the other hand, albumin behaved in the opposite manner and adsorption on high-curvature surfaces preserved the conformation better. It is known that fibrinogen adsorption promotes platelet adhesion,<sup>[34]</sup> but this is less true for denatured fibrinogen.<sup>[42]</sup> On the other hand, albumin adsorption can make surfaces less thrombogenic due to preventing of adsorption of other proteins.<sup>[41]</sup> This mechanism suggests that use of very small nanostructures could be beneficial for altering the adsorbed protein layer to be nonadherent to platelets.

#### 4. Discussion on Superhydrophobicity and Platelet Antiadhesion

Superhydrophobicity directly affects the effective area and hydrodynamic routes toward reducing platelet adhesion, and indirectly affects the other mechanisms. The Cassie state is a very promising way for achieving a less effective area for platelet adhesion. The air pocket not only protects against platelet adhesion, but also against protein adsorption. There is a wider possible parameter range to be utilized for effective-area reduction when the Cassie state is utilized since the parameter space of the Wenzel state is limited to having very narrow interstructure spacing, around 1  $\mu\text{m}$ . In addition, activated platelets that

assume more spread out morphologies could creep into even these narrow spaces.

There has been considerable effort in creating blood-repellent smooth surfaces<sup>[19]</sup> by utilizing hydrophilic and hydrophobic materials, typically polymers, or by immobilizing anticoagulants onto the surfaces. These efforts differ from the approach of SHB surfaces. In the case of the smooth surfaces, the goal has been to find a material that, through its surface chemical properties, prevents or alters protein adsorption or platelet adsorption/activation. The same is true of SHB surfaces, but, due to the reduced contact with a solid surface, new mechanisms specific to SHB surfaces emerge from the limited solid areas and alteration of flow effects across SHB surfaces. In fact, while an SHB surface has considerable roughness, it can be considered a smooth air/solid composite surface from the point of view of the liquid.

The Cassie state can cause significant slip over the surface.<sup>[47]</sup> Due to the lower viscosity of air compared to water, it could be expected that the hydrodynamic antiplatelet effects would be stronger on superhydrophobic surfaces as opposed to micro- and nanostructured surfaces in the Wenzel state. It is known that increased shear stress can cause increased platelet adhesion<sup>[9]</sup> and that an SHB surface in the Cassie state reduces the shear stress.<sup>[28]</sup> It is also known that local gradients in shear rate can lead to thrombosis in the low-shear-rate region, especially in the context of a plaque or another obstacle that has increased shear rate in the front side and a region of reduced shear behind it.<sup>[9,10]</sup> As long as the Cassie state remains, an SHB surface should be effectively smooth from the point of view of the flow. Although the material itself can have significant microstructure, the flow only sees the top surface of the material and the plastron, which is relatively smooth, although at higher pressures the plastron can gain some microstructure. Furthermore, the flow rate very close to an SHB surface is not zero as for a smooth surface. This means that platelets have less time to interact with the surface. A micro- and nanostructured surface in the Wenzel state on the other hand has significant shear-rate gradients, as the flow inside the structures can be very slow. However, this geometry differs from that of a plaque. In fact, the shear-rate gradient of a microstructured surface in the Wenzel state was hypothesized to be even beneficial.<sup>[38]</sup>

Antiadhesive properties proposed for SHB surfaces have been studied in both static and dynamic experiments. While the antiadhesive mechanisms proposed for SHB surfaces have been shown to benefit from increased shear rates, the shear rate itself can affect the mechanism by altering the dominant soluble agonists involved.<sup>[9]</sup> Thus, the experiments should be carried out preferably in the correct experimental conditions (static, flow) for the application in mind and, for application-independent studies, both setups should be utilized.

The slip created by the Cassie state also decreases the hydrodynamic flow resistance and therefore reduces the pressure drop for a given flow rate. This is beneficial for devices that interact directly with blood circulation. On the other hand, the pressure required for the initial filling (from dry to wetted) is higher in the case of superhydrophobic surfaces due to the capillary pressure. There is a possibility of an air bubble (other than plastron itself) being trapped during the filling of SHB structures, especially into topographical features such as corners or

pits. These air bubbles could, in principle, be detached by shear forces from the surface causing an air embolism risk.

Another issue is whether the presence of air in the plastron can itself lead to activation of platelets. It has been demonstrated that hydrophobic polymers (e.g., polytetrafluoroethylene, silicone rubber) can lead to significantly more platelet activation when filled normally, as opposed to priming in a way that removes all air bubbles that could remain in the cracks and roughness of the hydrophobic polymer (Ward 1, Ward 2). This effect is stronger in the presence of proteins, but remains also in a system with minimal proteins. While the plastron is not identical to air bubbles trapped in crevices of random roughness, in both the cases, the blood will come into contact with air. It is plausible that contact with the plastron could also increase activation in the case of SHB surfaces, but other effects of the SHB toward less activation could overcome this effect. Indeed, reduced activation levels of SHB surfaces compared to planar controls have been observed even with the presence of the plastron.<sup>[31]</sup>

A direct comparison with and without air is difficult for SHB surfaces. One option would be to fill the plastron with an inert gas. Another would be to utilize the same surface (of the type shown in Figure 3b, right side) in both the Wenzel and Cassie states. Performing such a test should be possible since both the Cassie and Wenzel states can be stable (or metastable) on the same surface. This experiment would standardize the effective area and the sizes of uniform areas, but the hydrodynamic effects would be different.

The above discussion applies only when the surface sustains a Cassie state. Surface micro- and nanostructures will commonly lead to an increase in the static or advancing contact angle of a water droplet due to local lateral pinning effects of the triple-phase contact line.<sup>[48]</sup> However, once the sample is immersed in liquid, the lateral local pinning effects that determined the contact angle no longer apply. Because of this, small or even large changes in the contact angles alone are unlikely to be helpful for explaining obtained antithrombotic effects. Instead, if superhydrophobicity is invoked as an explanation, the Cassie state should be confirmed by showing that the surface has low contact angle hysteresis. This can be done by measuring the advancing and receding contact angles, by measuring the sliding angles with a specified liquid volume, or by direct optical observation of the plastron. If the fabrication method allows, the contact angles of a planar surface with the same surface chemistry should also be reported, as they can be helpful for separating topographical and chemical effects.

The stability of the Cassie state has been indicated as a key factor for platelet antiadhesion.<sup>[30]</sup> One big challenge for the field is the long-term stability of the Cassie state. The lifetime of the plastron is dependent on the structure and on the pressure, and can be up to many weeks.<sup>[49]</sup> Nanoscale structures can achieve critical transition pressures in the hundreds of kilopascals,<sup>[50]</sup> which is higher than the pressures in blood vessels. Nanoscale structures can be fragile and coatings utilized can deteriorate over long term in flow conditions,<sup>[51]</sup> although SHB surfaces that can tolerate pressures exceeding megapascals have been demonstrated.<sup>[24]</sup> The antifouling properties of superhydrophobic surfaces have been studied extensively in the context of marine biofouling,<sup>[52]</sup> but there are few, if any,

reports on long-term fouling (by proteins, lipids, or cells) of blood-contacting SHB surfaces. Even if there is no degradation or fouling of the surface, the lifetime can still be limited by the dissolving of the plastron into the surrounding liquid.<sup>[53]</sup> Currently, much more research is needed into the short- and long-term stability of the Cassie state in physiological conditions. Still, even if the Cassie state is only stable for a shorter time, there are applications that do not require long-term stability, such as microfluidic plasma separator devices.<sup>[54]</sup>

## 5. Recent Examples of Blood-Repellent Surfaces

Metallic materials are used in blood-contacting implants like vascular stents and valves. Titanium and stainless steel are common choices. Preparing superhydrophobic surfaces out of titanium is straightforward with anodic oxidation.<sup>[55]</sup> The resulting TiO<sub>2</sub> nanotubes (in the 100 nm diameter range) coated by a fluorinated layer greatly reduce the platelet adhesion from 77 per 5000 μm<sup>2</sup> on a planar reference to 1 per 5000 μm<sup>2</sup> on an SHB surface. Pseudopod formation was also prevented. Figure 4a shows various titania structures with fluorinated coatings,<sup>[30]</sup> which make the structured surfaces superhydrophobic. Figure 4b shows fluorescence microscopy of platelets on all of the surfaces. The coverage of the platelets is reduced from 81% to 14% between the planar and the SHB nanotube topography. Moradi et al.<sup>[35]</sup> fabricated superhydrophobic titanium and steel surfaces by laser ablation (Figure 4c), and these surfaces were tested for platelet antiadhesion with various surface chemistries. The most superhydrophobic out of these combinations were the carbonized and silanized cauliflower topographies. These same surfaces also showed remarkable reduction in the platelet coverage compared to both their planar counterparts and hydrophilic surfaces (Figure 4d). This shows that the two key parameters to obtaining superhydrophobicity: topography and surface chemistry, are both required for platelet antiadhesion of superhydrophobic surfaces.

Bark et al.<sup>[56]</sup> studied the effect of a superhydrophobic coating on a bileaflet mechanical heart valve. The surface treatment applied on pyrolytic carbon and glass surfaces was a commercial Ultra-Ever Dry spray coating. The microstructure sizes were 10–50 μm. A receding contact angle of 160° was obtained with 4° contact angle hysteresis and 5° sliding angle (8–12 μL droplet size). The hierarchical SHB coating “eliminated” both platelet and leukocyte adhesion on the surfaces. High, but not physiologically excessive, shear stress was observed in fluid dynamics simulations. Platelet adhesion to heart-valve surfaces has also been reduced through the use of superhydrophobic hierarchically rough PDMS surfaces (static contact angle 164°).<sup>[57]</sup> Magnesium is biodegradable and can be made superhydrophobic by a simple sulfuric acid and hydrogen peroxide etching process and stearic acid surface treatment.<sup>[58]</sup> Reduction by a factor of 20 in platelet adhesion was observed by applying a superhydrophobic treatment on a magnesium alloy that is used for vascular stents.

Superhydrophobic surfaces were utilized in a plasma separator device.<sup>[54]</sup> The superhydrophobicity was achieved by applying a commercial Neverwet spray-on coating on top of a 3D printed large-scale micropillar array (500 μm size scale)

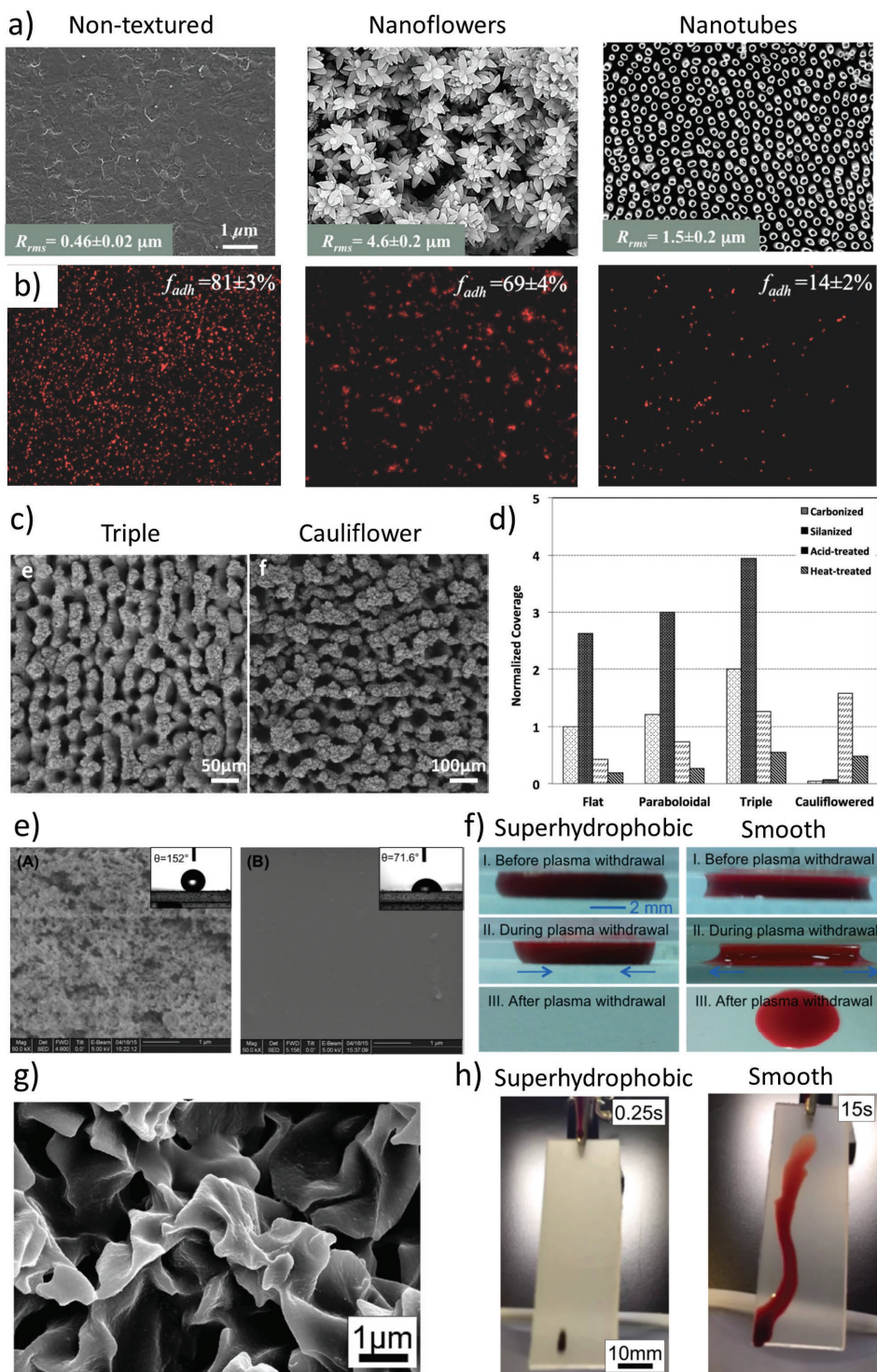


**Figure 4.** Recent examples of blood-repellent superhydrophobic surfaces. a) Planar and textured fluorinated titania surfaces. b) Fluorescence images showing the platelet coverage on the fluorinated titania surfaces. a,b) Adapted with permission.<sup>[30]</sup> Copyright 2016, Wiley-VCH. c) Scanning electron microscopy images of the laser-ablated titanium surfaces. d) Platelet adhesion coverage on laser-ablated titanium surfaces. The carbonized and silanized surfaces have hydrophobic surface chemistries. c,d) Adapted with permission.<sup>[35]</sup> Copyright 2016, American Chemical Society. e) Planar and superhydrophobic plasma separator surfaces. The superhydrophobic surface is made from commercial Neverwet. f) Operation of superhydrophobic and reference plasma separators. e,f) Adapted with permission.<sup>[54]</sup> Copyright 2015, Royal Society of Chemistry. g) Roll-to-roll fabricated superhydrophobic plastic. h) Blood droplet rolling on superhydrophobic plastic and sliding on planar plastic. g,h) Adapted with permission.<sup>[59]</sup> Copyright 2017, Wiley-VCH.

(Figure 4e). The SHB coating prevented blood clotting and reduced hemolysis and biomolecular adsorption. Figure 4f shows the operation of the device with and without the SHB coating, clearly demonstrating a blood clot on the uncoated device.

Nokes et al.<sup>[59]</sup> reported a large-scale manufacturing process of blood-repellent SHB polymer surfaces (Figure 4g) by a shrink-based roll-to-roll embossing. The resulting films display contact angles in excess of 150° for blood, urine, and saliva, and sliding angles below 10°. The volume of blood remaining on the surface after a 200 µL blood droplet had slid off a surface at a 30° angle was reduced from 80% on a flat surface to 2% on the SHB surface (Figure 4f). Blood coagulation was assessed by measuring the fibrin clot area, which showed significant onset delay compared with a flat reference. The polymers sheets were flexible, which allowed them to be rolled into tubes.

SLIPS were utilized for in vitro as well as in vivo studies of antithrombogenicity.<sup>[26]</sup> In vitro studies performed by coated medical-grade poly(vinyl chloride) tubing showed that SLIPS reduced the thrombus weight fourfold compared to reference tubes. A porcine femoral arteriovenous shunt model was used to assess thrombosis reduction in vivo. All of the SLIPS-coated circuits remained unobstructed for 8 h, even without heparin, while four out of five of the control circuits became occluded.

## 6. Conclusions

Blood-repellency based on superhydrophobic surfaces has shown promise in numerous studies and could be a new way toward antithrombic surfaces compared to the commonly utilized smooth surfaces. Several different mechanisms have been proposed, but the full picture of the effect of the topography and the role of superhydrophobicity is not yet clear. A typical superhydrophobic surface, composed of a nanoscale topography and a hydrophobic surface chemistry, would have less overall area for platelet adhesion and uniform adhesion areas smaller than platelet-sized. At the same time, the surface would be expected to exhibit slip and possibly to induce an altered protein conformation upon adsorption. These effects thus tend to be interwoven, which makes mechanistic studies more difficult, unless specific surface design steps are taken to disentangle them. At the same time, having multiple different protective effects rising from the same surface could be the critical requirement for robust blood repellency. Two key suggestions for further mechanistic studies can be made. First, it is critical to study and report whether the experiments happened in the Cassie or the Wenzel state, as most of the mechanisms are very different in these two cases. Notably, just a single high static contact angle is not enough to separate between these two states. Advancing and receding contact angles, sliding angles, or direct observation of the plastron (by reflection of light) are required. Second, whenever possible, studies should be performed in physiologically relevant flow conditions in addition to static conditions.

So far, some impressive results have been obtained in, for example, the reduction of the number of platelets adherent on the surface per unit area or reduced hemolysis. However, these results have almost exclusively been obtained in in vitro studies. In vivo results of superhydrophobic blood-repellent

materials are almost completely missing. The medical safety aspects are thus still largely unknown. One of the main challenges is the long-term stability of the superhydrophobic state in physiological conditions, as the trapped air layer tends to dissolve slowly into water. Another challenge is to develop fabrication processes that are suitable for implantable materials and complex components such as tubes or stents, as currently, most superhydrophobic surfaces are planar silicon, glass, polymer, or metal surfaces with only one side coated. Progress toward the long-term goal of implantable blood-contacting medical devices requires these aspects to be solved. However, even in the current state, ex vivo applications that benefit from lossless blood handling can already be realized.

## Acknowledgements

Funding from the Academy of Finland (#297360) and the Finnish Funding Agency for Innovation (#211679) is acknowledged. R.H.A.R. acknowledges the European Research Council for funding the Consolidator Grant SuperRepel (grant agreement no 725513). Expert help from Sole Lätti in graphical illustration is acknowledged.

## Conflict of Interest

The authors declare no conflict of interest.

## Keywords

antithrombogenic, blood-compatible, blood-repellent, nanostructures, superhydrophobic

Received: September 6, 2017

Revised: November 9, 2017

Published online:

- [1] A. C. Lima, J. F. Mano, *Nanomedicine* **2015**, *10*, 103.
- [2] A. C. Lima, J. F. Mano, *Nanomedicine* **2015**, *10*, 271.
- [3] I. Akin, H. Schneider, H. Ince, S. Kische, T. C. Rehders, T. Chatterjee, C. A. Nienaber, *Herz* **2011**, *36*, 190.
- [4] S. Pacelli, V. Manoharan, A. Desalvo, N. Lomis, K. S. Jodha, S. Prakash, A. Paul, *J. Mater. Chem. B* **2016**, *4*, 1586.
- [5] X. Liu, L. Yuan, D. Li, Z. Tang, Y. Wang, G. Chen, H. Chen, J. L. Brash, *J. Mater. Chem. B* **2014**, *2*, 5718.
- [6] M. B. Gorbet, M. V. Sefton, *Biomaterials* **2004**, *25*, 5681.
- [7] J. Petäjä, *Thromb. Res.* **2011**, *127*, S34.
- [8] F. Gaertner, S. Massberg, *Semin. Immunol.* **2016**, *28*, 561.
- [9] S. P. Jackson, W. S. Nesbitt, E. Westein, *J. Thromb. Haemostasis* **2009**, *7*, 17.
- [10] W. S. Nesbitt, E. Westein, F. J. Tovar-Lopez, E. Tolouei, A. Mitchell, J. Fu, J. Carberry, A. Fouras, S. P. Jackson, *Nat. Med.* **2009**, *15*, 665.
- [11] M.-F. Tsoi, C.-L. Cheung, T. T. Cheung, I. C.-K. Wong, C. R. Kumana, H.-F. Tse, B. M.-Y. Cheung, *Sci. Rep.* **2015**, *5*, 13204.
- [12] K. Aksu, A. Donmez, G. Keser, *Curr. Pharm. Des.* **2012**, *18*, 1478.
- [13] R. De Caterina, E. D'Ugo, P. Libby, *Thromb. Haemostasis* **2016**, *116*, 1012.
- [14] Z. M. Ruggeri, G. L. Mendolicchio, *Circ. Res.* **2007**, *100*, 1673.
- [15] D. Varga-Szabo, I. Pleines, B. Nieswandt, *Arterioscler., Thromb., Vasc. Biol.* **2008**, *28*, 403.

- [16] B. Estevez, X. Du, *Physiology* **2017**, 32, 162.
- [17] F. Franchi, D. J. Angiolillo, *Nat. Rev. Cardiol.* **2014**, 12, 30.
- [18] E. Salimi, A. Ghaee, A. F. Ismail, M. H. D. Othman, G. P. Sean, *Macromol. Mater. Eng.* **2016**, 301, 771.
- [19] B. D. Ratner, *Biomaterials* **2007**, 28, 5144.
- [20] E. J. Falde, S. T. Yohe, Y. L. Colson, M. W. Grinstaff, *Biomaterials* **2016**, 104, 87.
- [21] G. Wen, Z. Guo, W. Liu, *Nanoscale* **2017**, 9, 3338.
- [22] A. Marmur, in *Non-wettable Surfaces: Theory, Preparations and Applications* (Eds: R. H. A. Ras, A. Marmur), Royal Society of Chemistry, London, UK **2017**, Ch. 1.
- [23] V. Jokinen, P. Suvanto, A. R. Garapaty, J. Lyytinen, J. Koskinen, S. Franssila, *Colloids Surf., A* **2013**, 434, 207.
- [24] L. R. J. Scarratt, U. Steiner, C. Neto, *Adv. Colloid Interface Sci.* **2017**, 246, 133.
- [25] T. Verho, C. Bower, P. Andrew, S. Franssila, O. Ikkala, R. H. A. Ras, *Adv. Mater.* **2011**, 23, 673.
- [26] D. C. Leslie, A. Waterhouse, J. B. Berthet, T. M. Valentin, A. L. Watters, A. Jain, P. Kim, B. D. Hatton, A. Nedder, K. Donovan, E. H. Super, C. Howell, C. P. Johnson, T. L. Vu, D. E. Bolgen, S. Rifai, A. R. Hansen, M. Aizenberg, M. Super, J. Aizenberg, D. E. Ingber, *Nat. Biotechnol.* **2014**, 32, 1134.
- [27] C. Lee, C.-J. Kim, *Langmuir* **2009**, 25, 12812.
- [28] R. J. Daniello, N. E. Waterhouse, J. P. Rothstein, *Phys. Fluids* **2009**, 21, 085103.
- [29] D. M. Huang, C. Cottin-Bizonne, C. Ybert, L. Bocquet, *Phys. Rev. Lett.* **2008**, 101, 064503.
- [30] S. Movafaghi, V. Leszczak, W. Wang, J. A. Sorkin, L. P. Dasi, K. C. Popat, A. K. Kota, *Adv. Healthcare Mater.* **2017**, 6, 1600717.
- [31] T. Sun, H. Tan, D. Han, Q. Fu, L. Jiang, *Small* **2005**, 1, 959.
- [32] K. R. Milner, A. J. Snyder, C. A. Siedlecki, *J. Biomed. Mater. Res., Part A* **2006**, 76A, 561.
- [33] Y. Ding, Y. Leng, N. Huang, P. Yang, X. Lu, X. Ge, F. Ren, K. Wang, L. Lei, X. Guo, *J. Biomed. Mater. Res., Part A* **2013**, 101A, 622.
- [34] L. B. Koh, I. Rodriguez, S. S. Venkatraman, *Biomaterials* **2010**, 31, 1533.
- [35] S. Moradi, N. Hadjesfandiari, S. F. Toosi, J. N. Kizhakkedathu, S. G. Hatzikiriakos, *ACS Appl. Mater. Interfaces* **2016**, 8, 17631.
- [36] L. Chen, D. Han, L. Jiang, *Colloids Surf., B* **2011**, 85, 2.
- [37] H. Fan, P. Chen, R. Qi, J. Zhai, J. Wang, L. Chen, L. Chen, Q. Sun, Y. Song, D. Han, L. Jiang, *Small* **2009**, 5, 2144.
- [38] T. T. Pham, S. Wiedemeier, S. Maenz, G. Gastrock, U. Settmacher, K. D. Jandt, J. Zanow, C. Lüdecke, J. Bossert, *Colloids Surf., B* **2016**, 145, 502.
- [39] Y. Koc, A. J. de Mello, G. McHale, M. I. Newton, P. Roach, N. J. Shirtcliffe, *Lab Chip* **2008**, 8, 582.
- [40] P. Roach, D. Farrar, C. C. Perry, *J. Am. Chem. Soc.* **2006**, 128, 3939.
- [41] E. Luong-Van, I. Rodriguez, H. Y. Low, N. Elmouelhi, B. Lowenhaupt, S. Natarajan, C. T. Lim, R. Prajapati, M. Vyakarnam, K. Cooper, *J. Mater. Res.* **2013**, 28, 165.
- [42] G. A. Skarja, J. L. Brash, P. Bishop, K. A. Woodhouse, *Biomaterials* **1998**, 19, 2129.
- [43] T. N. Zaidi, L. V. McIntire, D. H. Farrell, P. Thiagarajan, *Blood* **1996**, 88, 2967.
- [44] B. J. Folie, L. V. McIntire, *Biophys. J.* **1989**, 56, 1121.
- [45] E. Fressinaud, K. S. Sakariassen, C. Rothschild, H. R. Baumgartner, D. Meyer, *Blood* **1992**, 80, 988.
- [46] R. Ramachandran, N. Maani, V. L. Rayz, M. Nosonovsky, *Philos. Trans. R. Soc., A* **2016**, 374, 20160133.
- [47] C.-H. Choi, C.-J. Kim, *Phys. Rev. Lett.* **2006**, 96, 066001.
- [48] V. Jokinen, L. Sainiemi, S. Franssila, *Langmuir* **2011**, 27, 7314.
- [49] R. Poetes, K. Holtzmann, K. Franze, U. Steiner, *Phys. Rev. Lett.* **2010**, 105, 166104.
- [50] Y. Su, B. Ji, K. Zhang, H. Gao, Y. Huang, K. Hwang, *Langmuir* **2010**, 26, 4984.
- [51] M. A. Samaha, H. V. Tafreshi, M. Gad-el-Hak, *Langmuir* **2012**, 28, 9759.
- [52] J. Genzer, K. Efimenko, *Biofouling* **2006**, 22, 339.
- [53] J. Xue, L. Pengyu, L. Hao, D. Huiling, *Appl. Mech. Rev.* **2016**, 68, 030803.
- [54] C. Liu, S.-C. Liao, J. Song, M. G. Mauk, X. Li, G. Wu, D. Ge, R. M. Greenberg, S. Yang, H. H. Bau, *Lab Chip* **2016**, 16, 553.
- [55] Y. Yang, Y. Lai, Q. Zhang, K. Wu, L. Zhang, C. Lin, P. Tang, *Colloids Surf., B* **2010**, 79, 309.
- [56] D. L. Bark, H. Vahabi, H. Bui, S. Movafaghi, B. Moore, A. K. Kota, K. Popat, L. P. Dasi, *Ann. Biomed. Eng.* **2017**, 45, 452.
- [57] X. Ye, Y. Shao, M. Zhou, J. Li, L. Cai, *Appl. Surf. Sci.* **2009**, 255, 6686.
- [58] P. Wan, J. Wu, L. Tan, B. Zhang, K. Yang, *Mater. Sci. Eng., C* **2013**, 33, 2885.
- [59] J. M. Nokes, R. Liedert, M. Y. Kim, A. Siddiqui, M. Chu, E. K. Lee, M. Khine, *Adv. Healthcare Mater.* **2016**, 5, 593.